Extraction of the Landing Point of the Bucket on the Stockpile

야적파일위의 버킷 착지점 추출

Chintae Choi, Hyunsik Ahn, Kwanhee Lee and Kitae Shin
(최 진 태, 안 현 식, 이 관 희, 신 기 태)

요 약 : 철강석 또는 석탄의 적치장에서는 이들 원석을 퍼내어 용광로로 보내주는 불출기(reclaimer)가 사용되고 있다. 불출기를 자동화하려면 야적파일에 불출용 회전 버킷(bucket)을 자동착지시키는 방법이 요구된다. 본 논문에서는 야적 파일 표면위의 버킷 착지점을 추출하는 방법을 제시한다. 이 방법은 파일의 3차원 형상 검출, 파일의 등고선 추출, 불출기의 역기구학해의 도출 및 착지점 추출 알고리즘으로 이루어진다. 파일의 3차원 형상과 거리를 측정하기 위한 3차원 형상 검출기가 2차원 레이저 검출기에 수평 주사(scanning)용 모터를 부착하여 개발하였고, 다 단계의 영상처리를 통해 버킷이 작업할 수 있도록 파일의 작업 등고선을 추출하였다. 불출기가 회전 버킷에 의해 기구학적으로 여유자유도로 이루어 졌음을 보였으며, 역기구학 해를 구하는 방법을 아울러 제시하였다. 그리고 버킷의 착지점을 과부하 방지와 단위 시간당 생산성을 최대화하는 성능기준에 근거하여 구하였다. 또한 개발된 시스템을 제철소 원석 야적장의 불출기에 설치 시험하여 타당성을 입증하였다.

Keywords : reclaimer, bucket, laser scanner, image processing, inverse kinematics, landing point, contour map

I. Introduction

In a steel company, stock yards contain piles of raw ore for later transfer to the blast furnaces at a scheduled time. In managing the piles of raw ore, reclaimers are used to dig out the raw ore and put it on the conveyer belt for transferring it to the blast furnaces. A reclaimer is very large, about 25 meters high, 50meters in length, and looks like a large crane. It has a 45 meters boom and a rotating disk with buckets at the end point of the boom for scooping raw ore as shown in Fig. 1. It has three degrees of free motion; a linear translation axis on the rail, a slewing axis and a pitching axis of the boom for approaching the pile. Generally, the reclaiming process consists of 2-stage operations: landing the reclaimer buckets on the surface of the pile and slewing the boom with the rotating buckets while the translation and pitching axes are fixed for easy and safe reclaiming job management. After slewing from the starting point to the end point, the reclaimer translates about 30cm for the next slewing. The pitching angle should be altered to change the digging level. Until now, landing operations have been done by remote control of well-experienced workers with the aid of some video cameras attached to the reclaimer.

The worker moves the three axes of the reclaimer by handling joysticks watching with the monitor in the main control room. However, the operation is not easy, because the image on the monitor cannot show the exact shape of the pile at night or bad weather. If the reclaimer collides with the pile or another machine, the reclaimer can cause serious problems. So it is necessary to develop an automation system for the reclaimer.

접수일자 : 1996. 10. 7., 수정완료 : 1998. 3. 20.
최진태, 안현식, 이관희, 신기태 : 포항산업과학연구원(RIST)

The most important function of the autonomous reclaimer is to detect a landing point on the surface of the pile and let the buckets land on it automatically without collision. The landing operation has been an obstacle to the full automation system for the material handling in the stock yards.

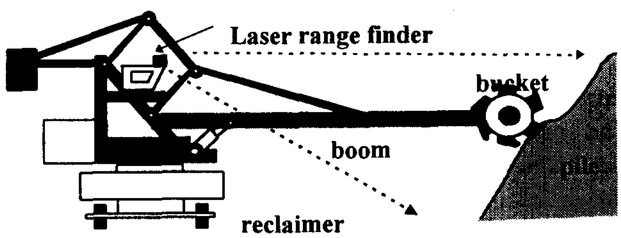

Fig. 1. Reclaimer approaching the pile.

In this paper, an automatic landing method of the reclaimer is proposed. To the best knowledge of the authors no published results for extraction of the landing point of the bucket on the stockpile or other related subjects are found in the literature yet. It is assumed that overload occurs in the buckets if the buckets dig ore more deeply in the pile than the prescribed depth of the bucket in the slewing operation. If the buckets are deeply embedded in the pile, it can not dig out ore. Therefore the operation has to be stopped because of severe overload. To detect the shape of the pile, a 3-dimensional range finder, which consists of a 2-dimensional scanner and an additional joint, is made and is installed on the roof of the reclaimer[1][2].

A height map is obtained from the acquired range data of an ore pile and a contour map for the pile is obtained through some image processing steps[3]. The

contour lines in the map are the job paths on which the buckets of the reclaimer can dig out the ore. Possible landing points are defined as ones that do not bring about the overload in the slewing operation.
An efficientl landing point in the contour line is determined so that the overload problem does not occur in the slewing operation and digging efficiency is maximized, simultaneously. The algorithm for searching the efficient landing point needs an inverse kinematics solution for the reclaimer. Since the rotating buckets at the end of the boom is considered as the end-effector with one degree of freedom, the reclaimer kinematics has redundant freedom. To solve the problem of the inverse kinematics, a constraint equation was derived using the contact relationship with the surface of the pile. The automation system with a 3-dimensional range finder and automatic landing capability was fully applied to the reclaimer in the raw ore yard of the iron-making works and showed satisfactory results.

II. Range-finding system

To obtain three dimensional shape data of the pile, a laser range finder which has two scanning axes is used. The distance from the sensor to the target pile is about 45 meters. The range finder has a large angle of view more than 70 degrees vertically and 270 degrees horizontally. It has a long-range point sensor, a rotating mirror for vertical scanning and a swivel joint for horizontal scanning. The point sensor is a time-of-flight laser range finder providing a range accuracy of +/- 3cm. The scanning speed of the sensor is 8 RPS with the sampling rate of 3 KHz.

When the host computer controlling the reclaimer receives a command from the supervisory computer, the reclaimer approaches the target pile and stops approximately at the proper position. Then, the range finder scans the front part of the pile after the reclaimer pause. The height and width of the pile are approximately 15m and 30m, respectively. Range data in the spherical coordinate system centered on the optical center of the range finder are acquired by encoding the step angles of the two rotating axes and detecting the depths of the points in the pile. The range data in the spherical coordinate system(r, α, γ) are transformed into the Cartesian coordinate system (x_s, y_s, z_s) as shown in Fig. 2.

$$x_s = r\sin\alpha\cos\gamma$$
$$z_s = r\cos\alpha \qquad (1)$$
$$y_s = r\sin\alpha\sin\gamma$$

The range data in the local coordinate system are transformed to the world coordinate system by geometric translation and rotation. A height map is generated by mapping the range data in the Cartesian coordinate system with the intensity value in the (U, V) image plane Fig. 3.
The unit steps of the (U, V) axes are selected according to the resolution of three dimensional profile data. Since the range data in the height map are expressed as sparsely scattered points from the optic center of the range finder, it is necessary to interpolate the range data to construct a three dimensional profile map. First, the two pixels which were computed from the neighboring range data through the scanning step of a rotating mirror are linearly interpolated. Second, linear interpolation through the swivel scanning axis is added like the mirror axis interpolation as shown in Fig. 4.

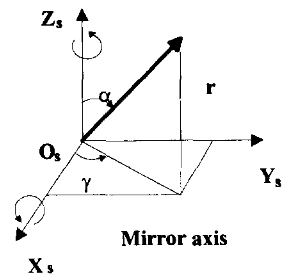

Fig. 2. Spherical coordinate system of the range finder.

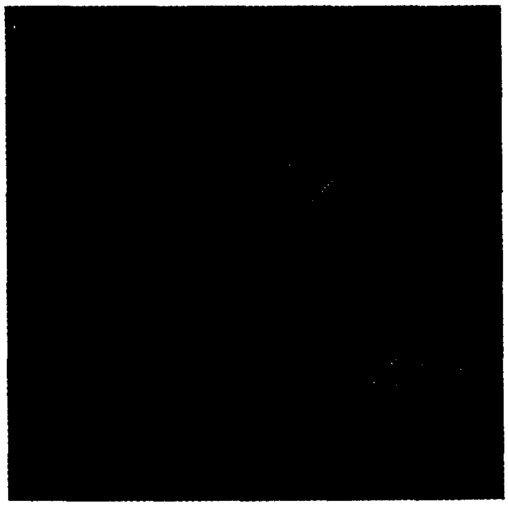
Fig. 3. Height map of range data array.


Fig. 4. Interpolated image of the height map.

In spite of interpolations, there may be many missing regions in the height map. The missing regions are merged linearly through the U or V axis. To merge the missing regions, the gray value of the pixels are examined along the V or U axis. The pixels which have no gray value are linearly interpolated by the gray values of the nearby pixels having gray level. Fig. 5 shows the merged image for the front part of the pile. After low pass filtering for noise reduction, the height map represents the 3 dimensional profile map meaning the real X, Y and Z coordinate of the object pile.

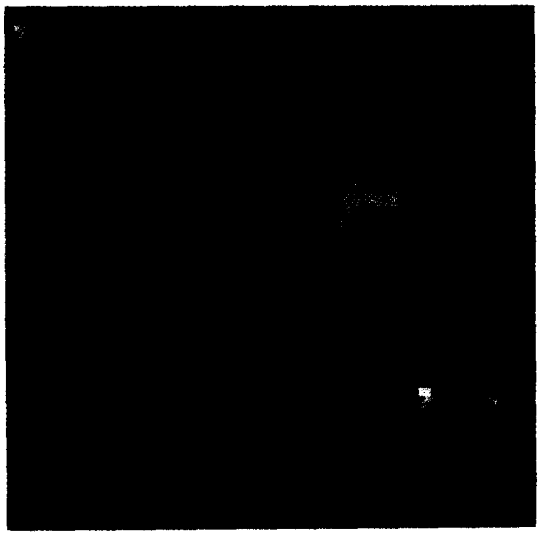

Fig. 5. Merged image of the height map.

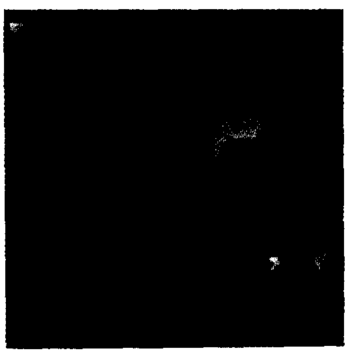

(a) Interpolation of the occluded region

(b) Merging of the occluded region

Fig. 6. Processings of the occuluded region.

The merged image still has occuluded regions having no gray values as shown in the figure. The regions can bring about problems that there exist more than one sliced image in the vicinity of the highest regions of the merged height map in the processing step of the contour line extraction. Therefore, the occuluded regions are interpolated with gradually decreasing gray value to the radial direction and are also merged to bear the final hight map for extracting contour lines. Fig. 6 shows the results of interpolation and merging of the height map.

In the final image processing step, the contour lines for the landing height of the buckets are extracted. Sliced images corresponding to the contour lines are obtained by thresholding the height map from the prior image processing step. Since the back side of the sliced image consists of false data as results of some image processings and has nothing to do with determination of the landing point, it is cut out from the image. Fig. 7 illustrates the procedure for contour line extraction.

The highest point in the hight map and the center line of the horizontal scanning angle are obtained, respectively. Then, the split line which passes the highest point and perpendicularly crosses the center line is obtained. The rear region of the split line in the sliced image are excluded from consideration. A contour line is extracted from the edge points in the front side of the split line in the sliced image by using the edge following technique. Fig. 8 shows the extracted contour map.

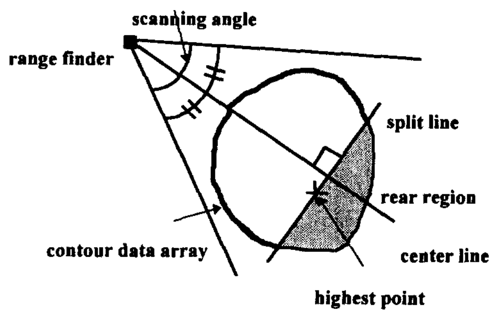

Fig. 7. Slice for the contour line.

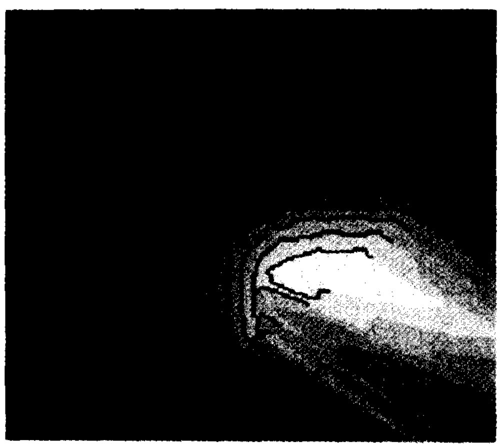

Fig. 8. Contour map for slewing operation.

III. Inverse kinematics of a reclaimer

The autonomous reclaimer is servoed in the joint-variable space, whereas the points on the pile are expressed in the world coordinate system. In order to control the position of the bucket to reach the points, the inverse kinematics solution should be solved. The disk-like end-effector has an action to produce another degree of freedom(DOF) when it lands on the pile. The DOF of the reclaimer is investigated with Fig. 9.

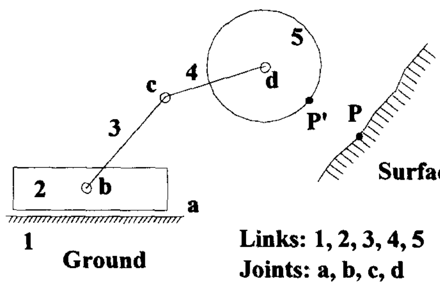

Fig. 9. The degree of freedom of the reclaimer.

The rectilinear motion of the main body moving on the rail is simplified as a prismatic joint (a) and the two rotational motions of the boom are simplified as revolute joints (b) and (c), respectively. It is also shown that the rotating disk at the end of the boom is connected by a revolute joint (d). Therefore the number of inputs to represent an arbitrary point P′ on the circumference of the disk is obtained by the following equation[4].

$$F=\lambda(l-j-1)+\sum_{i=1}^{j} f_i$$

where F = DOF of a mechanism, l = number of links, j = number of joints, f_i= DOF of the ith joint and λ = DOF that the mechanism can have in space. In the case of reclaimer l = 5, j = 4. Since each joint can have only one DOF, $\sum f_i=1+1+1+1=4$. λ = 6 due to the spatial motion of the reclaimer. Therefore the DOF of the reclaimer becomes F = 4. The necessity for finding the point P′ on the circumference of the disk becomes clear from the fact that the location of the point P on the pile determines P′.

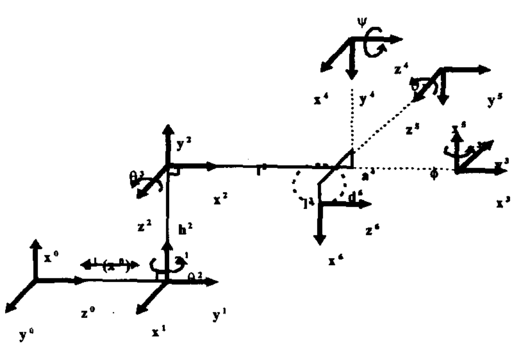

Fig. 10. Link assignment of the reclaimer.

Fig. 10 shows the assignment of link frames for the reclaimer. A Cartesian coordinate system $X_iY_iZ_i$ can be established for each link at its joint axis with the reference coordinate system $X_0Y_0Z_0$. ϕ and ψ are the fixed angles between the boom and the rotating disk by the mechanical structure. ψ helps the reclaimed ore fall onto the conveyor belt on the boom. Let (x_d, y_d, z_d) be a point on the pile. We would like to find the corresponding joint angles, θ_2 and θ_3 and translation distance d_1 of the reclaimer so that the bucket can be positioned as desired. θ_2 and θ_3 are the slewing and pitching angles of the boom, respectively. θ_r is an angle between z_6 and the contact point with the pile. It varies according to the shape of the pile, because the bucket should contact the pile at the one point. Therefore θ_r is another variable to be solved to determine d_1, θ_2 and θ_3.

With the link assignment, the kinematic equations are obtained as follows:

$$\begin{aligned} x_d = {} & \sin\theta_3\{l_3\cos\phi\sin\theta_r+\sin\phi(d_6\cos\psi\cos\theta_r)\} \\ & +\cos\theta_3(-l_3\cos\phi\cos\theta_r-d_6\sin\psi+a_4) \\ & +l_2\sin\theta_3+h_2 \end{aligned} \tag{2}$$

$$\begin{aligned} y_d = {} & -\sin\theta_2[\cos\theta_3\{l_3\cos\phi\sin\theta_r \\ & +\sin\phi(d_6\cos\psi\cos\theta_r)\}-\sin\theta_3(-l_3\cos\psi\cos\theta_r \\ & -d_6\sin\psi+a_4)+l_2\cos\theta_3]+\cos\theta_2\{\cos\phi \\ & (d_6\cos\psi-l_3\sin\psi\cos\theta_r)-l_3\sin\phi\sin\theta_r\} \end{aligned} \tag{3}$$

$$\begin{aligned} z_d = {} & \cos\theta_2[\cos\theta_3\{l_3\cos\phi\sin\theta_r+\sin\phi(d_6\cos\psi \\ & -l_3\sin\psi\cos\theta_r)\}-\sin\theta_3(-l_3\cos\psi\cos\theta_r \\ & -d_6\sin\psi+a_4)+l_2\cos\theta_3]+\sin\theta_2\{\cos\phi \\ & (d_6\cos\psi-l_3\sin\psi\cos\theta_r)-l_3\sin\phi\sin\theta_r\} \\ & +d_1. \end{aligned} \tag{4}$$

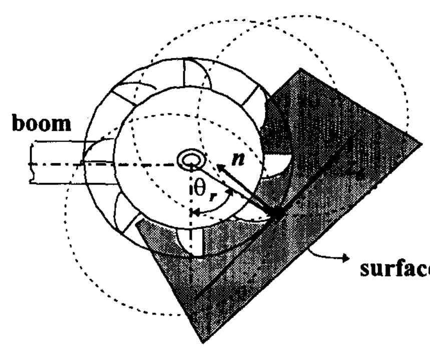

Fig. 11. Bucket on the estimated plane.

θ_r gives redundancy in the kinematics of the reclaimer as indicated in the above equation. Therefore, the number of the equations is fewer than that of the variables to be determined. The circles in Fig. 11 are the trajectories of the rotating buckets, which means that the way that the buckets can contact with the landing point exist infinitely. But the dotted circles mean that buckets are deeply embedded in the pile and both has already collapsed. Only the solid circle is desirable and θ_r is uniquely determined in this case. It gives us a constraint equation. It is derived from the fact that the circle should meet the surface of the pile at the one point.

In general, the piles have irregularly curved surfaces and it is very hard to extract the mathematical model of the surface. So the plane equation in the 3-dimensional space is more adequate in this application, because it is easily obtained using a projection method from the range data of the pile. A plane equation in the Cartesian coordinate can be expressed as follows:

$$n_x x + n_y y + n_z z = 1 \qquad (5)$$

where $\boldsymbol{n} = [\ n_x \ \ n_y \ \ n_z\ ]'$ is the normal vector of the plane. The reclaiming point and adjacent points ($\widehat{x_i}, \widehat{y_i}, \widehat{z_i}$) existing in the curved surface are selected to estimate the parameters of the plane equation. The points are determined as shown in Fig. 12. A landing point at the center of the curved plane and 8 adjacent points are chosen in this scheme.

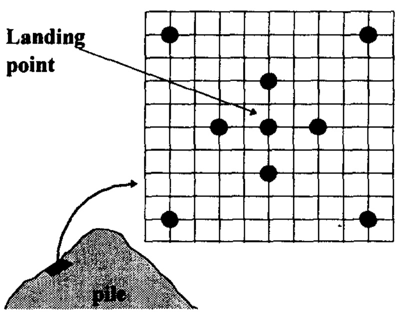

Fig. 12. Selected points in the surface.

Applying the points to the plane equation,

$$\begin{bmatrix} x_d & y_d & z_d \\ \widehat{x_1} & \widehat{y_1} & \widehat{z_1} \\ \vdots & \vdots & \vdots \\ \widehat{x_8} & \widehat{y_8} & \widehat{z_8} \end{bmatrix} \begin{bmatrix} n_x \\ n_y \\ n_z \end{bmatrix} = \begin{bmatrix} 1 \\ 1 \\ \vdots \\ 1 \end{bmatrix} \qquad (6)$$

Rewriting the above equation in a simpler form,

$$\boldsymbol{W} \cdot \boldsymbol{n} = \boldsymbol{u} \qquad (7)$$

where $\boldsymbol{u} = [1\ 1\ \cdots\ 1]'$. Since the points in the matrix $\boldsymbol{W}$ are different in the curved plane, there exists the pseudo-inverse of $\boldsymbol{W}$. The normal vector of the plane is given as a solution of the normal equation[5] which is

$$\boldsymbol{n} = (\boldsymbol{W}^T \boldsymbol{W})^{-1} \boldsymbol{W}^T \boldsymbol{u}. \qquad (8)$$

From the assignment of the link frames, $\boldsymbol{z_6} = [\,z_{6x}\ z_{6y}\ z_{6z}]'$ is obtained as follows:

$$\begin{aligned} z_{6x} &= \cos\theta_2(\cos\phi\sin\theta_r - \sin\phi\cos\theta_r) \\ &- \sin\theta_2(\cos\theta_3\sin\phi\sin\psi\sin\theta_r + \cos\phi\cos\theta_r) \\ &- \cos\psi\sin\theta_3\sin\theta_r \end{aligned} \qquad (9)$$

$$\begin{aligned} z_{6y} &= \cos\theta_2\{\cos\theta_3(\sin\phi\sin\psi\sin\theta_r + \cos\phi\cos\theta_r) \\ &- \cos\psi\sin\theta_3\sin\theta_r\} + \sin\theta_2(\cos\phi\sin\psi\sin\theta_r \\ &- \cos\phi\cos\theta_r) \end{aligned} \qquad (10)$$

$$\begin{aligned} z_{6z} &= \sin\theta_3(\sin\phi\sin\psi\sin\theta_r + \cos\phi\cos\theta_r) \\ &+ \cos\psi\cos\theta_3\sin\theta_r \end{aligned} \qquad (11)$$

In order that the circle of the rotating buckets meets the surface of the pile at one point, the vector $\boldsymbol{z_6}$ and $\boldsymbol{n}$ should make a right angle. Namely, The inner product of two vectors should be 0. Obtaining the inner product,

$$\begin{aligned} f(\theta_r) &= \boldsymbol{z}_6^T \cdot \boldsymbol{n} = z_{6x} \cdot n_x + z_{6y} \cdot n_y + z_{6z} \cdot n_z \\ &= n_x\{\sin\theta_3(\sin\phi\sin\psi\sin\theta_r + \cos\phi\cos\theta_r) \\ &\quad + \cos\psi\cos\theta_3\sin\theta_r\} \\ &\quad + n_y[\cos\theta_2(\cos\phi\sin\psi\sin\theta_r - \sin\phi\cos\theta_r) \\ &\quad - \sin\theta_2\{\cos\theta_3 \cdot (\sin\phi\sin\psi\sin\theta_r + \\ &\quad \cos\phi\cos\theta_r) - \cos\psi\sin\theta_3\sin\theta_r\}\,] \\ &\quad + n_z[\cos\theta_2\{\cos\theta_3(\sin\phi\sin\psi\sin\theta_r + \\ &\quad \cos\phi\cos\theta_r) - \cos\psi\sin\theta_3\sin\theta_r\} \\ &\quad + \sin\theta_2(\cos\phi\sin\psi\sin\theta_r - \sin\phi\cos\theta_r)] \\ &= 0 \end{aligned} \qquad (12)$$

The inverse kinematics problem can be solved with the forward kinematic equations and the constraint(12). Since the equation is highly coupled and nonlinear, analytical solutions are hard to obtain. Thus, the numerical method is used. Arranging (2) and (3),

$$x_d = \Delta_1\sin\theta_3 + \Delta_2\cos\theta_3 + h_2 \qquad (13)$$

$$y_d = -\Delta_1\sin\theta_2\cos\theta_3 + \Delta_2\sin\theta_2\sin\theta_3 + \Delta_3\cos\theta_2 \qquad (14)$$

where

$$\begin{aligned} \Delta_1 &= l_3\cos\phi\sin\theta_r + \sin\phi(d_6\cos\psi - l_3\sin\psi\cos\theta_r) \\ &+ l_2 \\ \Delta_2 &= -l_3\cos\psi\cos\theta_r - d_6\sin\psi + a_4 \\ \Delta_3 &= \cos\phi(d_6\cos\psi - l_3\sin\psi\cos\theta_r) - l_3\sin\phi\sin\theta_r. \end{aligned}$$

Since $\Delta_1, \Delta_2, \Delta_3$ are completely determined by θ_r, (13) is the equation of θ_r and θ_3. Rewriting the equation,

$$\begin{aligned} x_d - h_2 &= \Delta_1\sin\theta_3 + \Delta_2\cos\theta_3 \\ &= \sqrt{\Delta_1^2 + \Delta_2^2}\cos(\theta_3 - \beta) \end{aligned} \qquad (15)$$

where $\cos\beta = \Delta_1/\sqrt{\Delta_1^2+\Delta_2^2}$ and $\sin\beta = \Delta_2/\sqrt{\Delta_1^2+\Delta_2^2}$. Then, β is written as:

$$\beta = \pm\arctan(\Delta_2/\Delta_1) \qquad (16)$$

Dividing the both sides of (15) by $\sqrt{\Delta_1^2+\Delta_2^2}$ and arranging it with trigonometrical relation,

$$\cos(\theta_3 - \beta) = \frac{x_d - h_2}{\sqrt{\Delta_1^2 + \Delta_2^2}} \qquad (17)$$

$$\sin(\theta_3 - \beta) = \sqrt{\frac{\Delta_1^2 + \Delta_2^2 - (x_d - h_2)^2}{\Delta_1^2 + \Delta_2^2}} \qquad (18)$$

Using (17) and (18), θ_3 is written as follows:

$$\theta_3 = \arctan(\Delta_2/\Delta_1) \pm \arctan\left(\frac{\sqrt{\Delta_1^2+\Delta_2^2-(x_d-h_2)^2}}{x_d-h_2}\right) \quad (19)$$

θ_3 is determined with θ_r as indicated in (19). With the similar method, θ_2 is written as

$$\theta_2 = \pm\arctan\left(\frac{-\Delta_1\cos\theta_3+\Delta_2\sin\theta_3}{\Delta_3}\right) \pm\arctan\left(\frac{\sqrt{(-\Delta_1\cos\theta_3+\Delta_2\sin\theta_3)^2+\Delta_3^2-y_d^2}}{y_d}\right) \quad (20)$$

θ_2 is also obtained with θ_3 and θ_r. The constraint (12) is also rewritten as the function of θ_r by applying (19) and (20). The signs in the (19) and (20) are determined by kinematic configurations of the reclaimer.

The false position method[6] which is a kind of numerical method is used to obtain the joint angles. The initial value of θ_r is set between 0 and 90 degrees by considering the stock angle of the pile. With θ_2, θ_3 and θ_r, d_1 is obtained in the (4).

IV. Extraction of a landing pont

The most convex part of the pile is, in general, chosen as a landing point when well-experienced operators start to reclaim ore. The procedure of the reclaiming operation is as follows: first, the reclaimer approaches the pile so that the buckets can gently contact with the most convex point, then the buckets are rotated to prevent abrupt collision in front of the point and lastly, the slewing operation begins while the other joints are fixed.

To automate the reclaimer, the automatic landing method which can substitute the landing skill of the well-experienced operator is needed. In this paper, a method to determine a landing point is obtained. A landing point of the buckets should be determined so as not to allow overload problems when the slewing operation is done. Let d_t be the desired digging depth of the bucket into the pile. d_t is determined according to the specific gravities of the ore and reclaiming mass per hour, *etc.* It is assumed that overload happens in the buckets if the buckets dig ore more deeply in the pile than the prescribed depth of the bucket.

Fig. 13 shows the contour line of the pile and the slew arc which is the trajectory of the bucket in the slewing operation. The line consists of digitized points $p_i\,(i=1,\cdots,n)$. All points are assumed as possible landing points and its feasibility is investigated. If a point bring about overload, it is excluded from the set of candidates of the landing points.

Some points in the contour line are chosen as candidates for landing points by investigating the digging depth of the bucket when these pass through the pile in the slew operation. S is defined as a set of feasible landing points. The landing point which has the maximum slew angle is an efficient landing point, because the smaller slew angle causes frequent changes of slew direction and therefore productivity is lowered.

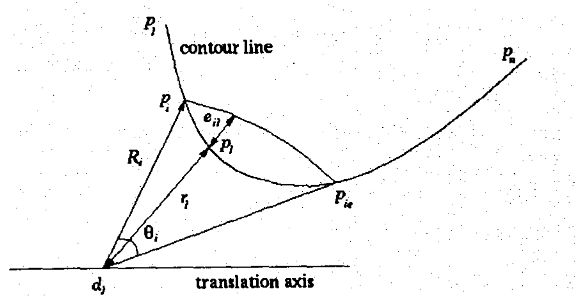

Fig. 13. Top view of the contour line and slew arc.

The algorithm is summarized as follows :

1) FOR $i=1$ TO n

a) Determine $d_1, \theta_2, \theta_3, \theta_r$ for the point p_i using the inverse kinematics.

b) The translation position d_1 is set to the slewing center for reclaiming.

c) An arc whose center is d_1 is drawn from p_i to p_{ie} which is the end point of slewing.

d) Let R_i define the radius of the arc which is the trajectory of the rotating buckets in the slewing operation.

e) Take all the points $p_l\,(l=1,\cdots,j)$ on the contour curve between p_i and p_{ie} for consideration.

f) FOR $l=1$ TO j

Calculate the distance r_l from d_1 to p_l. Calculate the absolute difference $e_{il}=|R_i-r_l|$ of R_i and r_l where e_{il} means the embedded depth of the buckets in the slewing operation.

g) ENDFOR l

h) Determine $e_i=\max\{e_{il} \mid l=1,\cdots,j\}$ where e_i is the maximum embedded depth when the slewing operation is done after taking p_i as the landing point.

i) IF $e_i \le d_t$ THEN p_i is chosen as a candidate point in which slewing operation can be done without overload. p_i becomes an element of the set S.

j) ELSE the point p_i is discarded.

2) ENDFOR i

3) Obtain $\theta_{\max}=\max\{\theta_i \mid p_i \in S\}$ θ_i which is an angle between the landing point and slew limit.

4) Obtain for the p_i's.

5) The point p_i for the $\theta_{\max}$ is chosen as the efficient landing point.

Fig. 14 shows the graphical display for the pile and reclaimer. The scanned pile data from the range finder are reconstructed for the workers to be able to see the shape of the pile by the 3-dimensional graphics. The reclaimer is drawn by animation techniques and the display of its on-line configuration is performed using the position data of the sensors in the joints. The contour line illustrates the reclaiming hight of the pile and the efficient landing point and slew limit are extracted from the above algorithm.

Fig. 14. Graphic display of the yard.

V. Conclusions

A 3-dimensional laser range finder is installed on the roof of the reclaimer to detect the ore pile. A height map is obtained from the acquired range data for an ore pile and a contour map for the pile is obtained through some image processing steps. All the points in the contour lines are examined to determine the landing point of the bucket. The efficient landing point is determined so that overload does not occur in the slewing operation and reclaiming efficiency is maximized. The algorithm for finding the landing point needs an inverse kinematics solution for the reclaimer. The reclaimer has a redundant joint due to the rotating buckets when they land on the pile. We also propose a method for solving the inverse kinematics of the reclaimer. The proposed algorithm has been successfully implemented to the reclaimer in the stockyards and a full-automation system is now being developed.

References

[1] V. E. Theodoracatos and D. E. Calkins, "A 3-D vision system model for automatic object surface sensing," *International Journal of Computer Vision*, vol. 11, no. 1, pp. 75-99, 1993.

[2] M. Asada, M. Kimura, Y. Taniguchi and Y. Shrai, "Dynamic integration of height maps into a 3D world representation from range image sequences," *International Journal of Computer Vision*, vol. 9, no. 1, pp. 31-53, 1992.

[3] D. Langer, J. K. Rosenblatt and M. Hebert, "A behavior-based system for off-round navigation," *IEEE Trans. Robotics and Automation*, vol. 10, no. 6, pp. 776-783, 1994.

[4] G. N. Sander and A. G. Erdman, *Advanced Mechanism Design: Analysis and Synthesis*, Prentice Hall, 1984.

[5] G. Strang, *Linear Algebra and Its Applications*, Harcourt Brace Jovanovich, Inc., 1988.

[6] S. C. Chapra and R. P. Canale, *Numerical Methods for Engineers*, McGraw-Hill, 1990.

최 진 태

제어 · 자동화 · 시스템공학 논문지 제 3권 제 2호 참조.

이 관 희

제어 · 자동화 · 시스템공학 논문지 제 3권 제 5호 참조.

안 현 식

제어 · 자동화 · 시스템공학 논문지 제 3권 제 5호 참조.

신 기 태

제어 · 자동화 · 시스템공학 논문지 제 3권 제 5호 참조.